Journal of Beijing Institute of Technology, 2021, Vol. 30, Suppl.1

Wafer Stage Modal Model Identification by Modified Vector Fitting Method

Xu Yang[1,2], Ming Zhang[1,2], Rong Cheng[1,2,✉], Yu Zhu[1,2] and Leijie Wang[1,2]

(1. State Key Laboratory of Tribology, Department of Mechanical Engineering, Tsinghua University, Beijing 100084, China; 2. Beijing Key Laboratory of Precision/Ultra-precision Manufacturing Equipments and Control, Tsinghua University, Beijing 100084, China)

Abstract: Vector fitting is modified in this study for the parametric identification of a model with an undamped rigid body mode in the frequency domain. The modal model of a six-degree-of-freedom (6DOF) wafer stage is identified using the modified vector fitting method. The modal model is typically fitted from the matrix fraction description (MFD) form of the transfer function, which increases the cost function. The vector fitting in frequency domain provides an approach to fitting the modal model directly from frequency response functions (FRFs) via a partial rational basis function, the poles of which can be obtained by pole relocation technology. The traditional vector fitting method is not applicable in identifying systems containing rigid body modes. The method is reformulated here and effectively applied for wafer stage identification. The accuracy of the fitted model is validated by control loop simulation.

Key words: system identification; vector fitting; wafer stage

CLC number: TP29 **Document code:** A **Article ID:** 1004-0579(2021)S1-0187-09

The wafer stage of lithography is a highly complex system which must perform exceedingly well to meet the increasingly stringent accuracy requirements for IC manufacturing, precision measurement, and other applications. The moving component of the wafer stage was once described as a rigid body and equipped with a specialized controller on its base[1]. More recent improvements in control accuracy have caused the flexible mode of wafer stage to limit the control bandwidth of the system, which in turn affects its capacity for suppressing disturbance[2]. The flexible dynamic frequency may also cross the bandwidth in future motion systems, so the flexible mode of the moving component must be properly taken into account. To improve the accuracy and speed of the wafer stage, existing controller design approaches for plants with flexible modes are usually based on input shaping[3], model inversing[4], dynamic decoupling[5], over-actuation[6], and inferential control[7]. The efficiency of these methods all rely on an accurate plant model.

Modal knowledge of the flexible system is dependent on knowledge of its structural dynamics, which may be gained by finite-element analysis[8]. However, the resonance frequency and damping ratio gathered by structural dynamic analysis are inherently inaccurate and must be updated by experimental data. Identification technology is a general method which can be used to obtain accurate motion system models[9]. The input and output of the acquired model represent the actuator and sensors, respectively, which renders any additional updating of the model unnecessary.

Received 2020-05-29
Supported by the National Natural Science Foundation of China (51677104)
✉ Author for correspondence, assistant professor, Ph.D.
E-mail: chengr@tsinghua.edu.cn
DOI: 10.15918/j.jbit1004-0579.20052

The frequency domain method is often applied to mitigate the disadvantages of time domain methods[10-11] including noise reduction, data reduction, and model quality. Frequency domain identification is selected for the purposes of this study. Generally, a transfer function in form of a coprime factorization would be fitted from the frequency response function (FRF) obtained by non-parametric identification procedure. The fitting process is called parametric identification. The objective of fitting is to minimize the cost function, which represents the error between the transfer function and FRF[10]. Sanathanan-Koerner (SK)[12], Gauss-Newton (GN)[13], and Instrumental-Variables (IV)[14] algorithms have been utilized for parametric identification. To mitigate the disturbance of flexible mode in wafer stage motion control, the modal displacement should be calculated as the feedback in control loop. Then the modal parameters including eigenvectors and damping ratio should be extracted from the transfer function, so the transfer function in form of MFD must be transformed to modal model. However, this process would cause an increase in cost value, which would lead to an inaccuracy in modal parameters.

A rational basis function containing pole pairs can be applied to fit modal model directly from the FRFs, as proposed by Gustavsen[15]. The rational basis function was obtained using pole location technology and the identification method is the so called vector fitting. However, the vector fitting proposed can not be applied on wafer stage identification because of the poles of rigid mode can not identified by poles location.

The main contribution of this work is that the vector fitting method is modified to be applicable to the identification of wafer stage systems containing rigid body modes. The proposed identification approach is explained in Section 3. Section 4 presents the results of a prototype wafer stage system experiment. The accuracy of the model was further validated through system simulation, as discussed in detail below.

1 Problem Statement

1.1 Modal modeling

The stage can be described as a linear-time-invariant (LTI) system. The system model can be characterized by the mass, stiffness, and damping matrices as well as the sensor and actuator locations[16]. In the nodal coordinates, the model can be represented using second-order matrix differential equations:

$$\begin{aligned} \boldsymbol{M}\ddot{\boldsymbol{q}} + \boldsymbol{D}\dot{\boldsymbol{q}} + \boldsymbol{K}\boldsymbol{q} &= \boldsymbol{B}_0 u \\ \boldsymbol{y} &= \boldsymbol{C}_{\mathrm{oq}}\boldsymbol{q} + \boldsymbol{C}_{\mathrm{ov}}\dot{\boldsymbol{q}} \end{aligned} \tag{1}$$

where $\boldsymbol{q}$ denotes the $n_{\mathrm{d}}\times 1$ displacement vector and n is the number of DOFs. $\boldsymbol{u}$ denotes the $n_{\mathrm{i}}\times 1$ input vector and y denotes the $n_{\mathrm{o}}\times 1$ output vector. $\boldsymbol{M}$, $\boldsymbol{D}$, and $\boldsymbol{K}$ are the mass matrix, damping matrix, and stiffness matrix, respectively, each with dimensions of $n_{\mathrm{d}}\times n_{\mathrm{d}}$. $\boldsymbol{B}_0$ is the $n_{\mathrm{d}}\times n_{\mathrm{i}}$ input matrix and $\boldsymbol{C}_{\mathrm{op}}$ and $\boldsymbol{C}_{\mathrm{ov}}$ denote the output displacement matrix and output velocity matrix with dimensions of $n_{\mathrm{o}}\times n_{\mathrm{d}}$, respectively. The variable $\boldsymbol{q}_{\mathrm{m}}$ can be introduced in the modal coordinates:

$$\boldsymbol{q} = \boldsymbol{\Phi}\boldsymbol{q}_{\mathrm{m}} \tag{2}$$

where $\boldsymbol{\Phi}$ is the modal matrix, which contains n natural modes. The differential equations in the nodal coordinates can be transformed to suit the modal coordinates:

$$\begin{aligned} \ddot{\boldsymbol{q}}_{\mathrm{m}} + 2\boldsymbol{Z}\boldsymbol{\Omega}\dot{\boldsymbol{q}}_{\mathrm{m}} + \boldsymbol{\Omega}^2\boldsymbol{q} &= \boldsymbol{B}_{\mathrm{m}}\boldsymbol{u} \\ \boldsymbol{y} &= \boldsymbol{C}_{\mathrm{mq}}\boldsymbol{q}_{\mathrm{m}} + \boldsymbol{C}_{\mathrm{mv}}\dot{\boldsymbol{q}}_{\mathrm{m}} \end{aligned} \tag{3}$$

The differential equation of each modal displacement is then

$$\begin{aligned} \ddot{q}_{\mathrm{m}i} + 2\zeta_i\omega_i\dot{q}_{\mathrm{m}i} + {\omega_i}^2 q_{\mathrm{m}i} &= \boldsymbol{b}_{\mathrm{m}i}\boldsymbol{u} \\ \boldsymbol{y} &= \boldsymbol{c}_{\mathrm{mq}i}q_{\mathrm{m}i} + \boldsymbol{c}_{\mathrm{mv}i}\dot{q}_{\mathrm{m}i} \end{aligned} \tag{4}$$

So the transfer function of the ith mode can be obtained as follows

$$G_i(s) = \frac{(c_{\mathrm{mq}i} + c_{\mathrm{mv}i}s)\, b_{\mathrm{m}i}}{s^2 + 2\zeta_i\omega_i s + {\omega_i}^2} \tag{5}$$

The whole system model is the sum of the

modal transfer functions

$$G(s)=\sum G_i(s) \tag{6}$$

The transfer function (Eq. (5)) also can be written as a state space model

$$\begin{aligned}
&\dot{\boldsymbol{x}}_{\mathrm{m}i}=\boldsymbol{A}_{\mathrm{m}i}\boldsymbol{x}_i+\boldsymbol{B}_{\mathrm{m}i}\boldsymbol{u}\\
&\boldsymbol{y}_i=\boldsymbol{C}_{\mathrm{m}i}\boldsymbol{x}_i\\
&\boldsymbol{A}_{\mathrm{m}i}=\begin{bmatrix}0 & 1\\ -\omega_i^2 & -2\zeta_i\omega_i\end{bmatrix}\\
&\boldsymbol{B}_{\mathrm{m}i}=\begin{bmatrix}0\\ \boldsymbol{b}_{\mathrm{m}i}\end{bmatrix}\\
&\boldsymbol{C}_{\mathrm{m}i}=\begin{bmatrix}\boldsymbol{c}_{\mathrm{mq}i} & \boldsymbol{c}_{\mathrm{mv}i}\end{bmatrix}
\end{aligned} \tag{7}$$

and the whole state space model is composed by

$$\begin{aligned}
&\boldsymbol{A}_{\mathrm{m}}=\mathrm{diag}\left(\boldsymbol{A}_{\mathrm{m}i}\right)\\
&\boldsymbol{B}_{\mathrm{m}i}=\begin{bmatrix}\boldsymbol{B}_{\mathrm{m}1}\\ \boldsymbol{B}_{\mathrm{m}2}\\ \vdots\\ \boldsymbol{B}_{\mathrm{m}n}\end{bmatrix}\\
&\boldsymbol{C}_{\mathrm{m}i}=\begin{bmatrix}\boldsymbol{C}_{\mathrm{m}1} & \boldsymbol{C}_{\mathrm{m}2} & \cdots & \boldsymbol{C}_{\mathrm{m}n}\end{bmatrix}
\end{aligned} \tag{8}$$

Variable ω_i (Eqs. (5) (7)) would be zero in the rigid body part of both the transfer function and state space model. In addition, c_{mv} can be set to 0 as the output is measured by displacement sensors.

1.2 Vector fitting

In this study, the modal model of the system is fitted directly from the FRFs. Then the partial rational fractions basis function is used in the following form to improve the numerical conditioning of the iterative algorithm:

$$\phi_{\mathrm{p}}=\frac{1}{1+a_{\mathrm{p}}} \tag{9}$$

The poles of the basis function were also the poles of the modal model to be fitted, which were obtained using the relocation technology proposed by Gustavsen[15]. A given order transfer function can be approximated by a ratio of two polynomials[15]:

$$f(s)\approx\frac{a_0+a_1s+a_2s^2+\cdots+a_Ns^N}{b_0+b_1s+b_2s^2+\cdots+b_Ns^N}\approx\sum_{n=1}^{N}\frac{c_n}{s-a_n}+d+sh \tag{10}$$

where a_n and c_n (right term) are complex conjugate pairs. The identification problem serves to estimate a_n, c_n, d, and h in the right term, which is obviously a nonlinear problem as a_n is unknown in the dominator. The first stage of the fitting process is to identify the poles via pole relocation. The response function $f(s)$ is then multiplied with a rational function $\sigma(s)$ with initial poles $\bar{a}$:

$$\begin{bmatrix}\sigma(s)f(s)\\ \sigma(s)\end{bmatrix}\approx\begin{bmatrix}\sum_{n=1}^{N}\frac{c_n}{s-\bar{a}}+d+sh\\ \sum_{n=1}^{N}\frac{\tilde{c}_n}{s-\bar{a}}+1\end{bmatrix} \tag{11}$$

and the residues of Eq. (11) are calculated by solving the following problem

$$\left(\sum_{n=1}^{N}\frac{c_n}{s-\bar{a}}+d+sh\right)-\left(\sum_{n=1}^{N}\frac{\tilde{c}_n}{s-\bar{a}}\right)f(s)=f(s) \tag{12}$$

The poles of $f(s)$ are equal to the zeros of $\sigma(s)$ at this point[16]. The second stage of the vector fitting serves to calculate the residues of $f(s)$. Eq. (10) can be transferred into a linear problem with the known poles of $f(s)$. Vector fitting thus resolves the linear least squares problem using the rational basis function, which can be considered a reformulation of the SK algorithm.

However, the chosen initial approximation of $f(s)$ affects the fitting results if the transfer response contains an undamped rigid body mode. Consider a single-input, single-output transfer function in the following form

$$f(s)=\frac{1}{6s^2}+\frac{0.2}{s^2+62.831\,9s+9.869\,6\times10^6} \tag{13}$$

where the first term is the rigid mode and the second term is the flexible mode. If Eq. (10) is chosen as the approximation of the transfer function, the pole set calculated in the first stage would contain a pair of poles out of the frequency range of FRF. This is because the undamped rigid body mode cannot be described using the partial rational function as shown in Eq. (10). The FRF and model obtained using vector fitting are shown in Fig. 1. The green line is the Bode diagram of the transfer function fit-

ted from the model without a rigid mode. The vector fitting should be modified to make it applicable to the model with a rigid body.

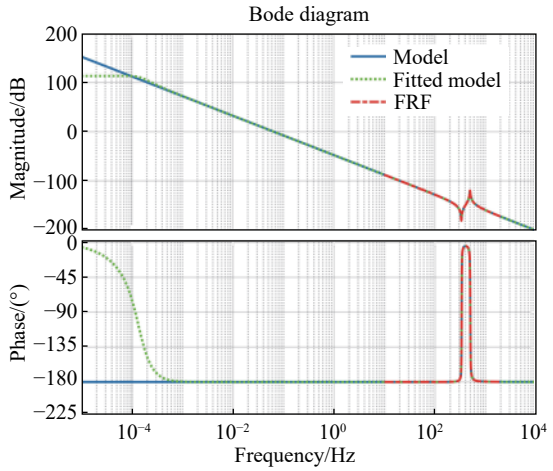

Fig. 1 Bode diagram of transfer function obtained using vector fitting

2 Proposed Modified Vector Fitting Method

2.1 Modified vector fitting

The constraint of the transfer function should be enforced by factorizing the rigid body part out of the model description.

$$f(s)=\frac{1}{ms^2}+\frac{\alpha}{s^2+2\xi\omega s+\omega^2}=\frac{1}{ms^2}+\frac{c}{s-a}+\frac{c^*}{s-a^*} \tag{14}$$

$\sigma(s)$ is multiplied on $f(s)$ to obtain the following

$$\begin{bmatrix}\sigma(s)f(s)\\ \sigma(s)\end{bmatrix}\approx\begin{bmatrix}\sum_{n=1}^{N}\frac{c_n}{s-\bar{a}}+d\\ \sum_{n=1}^{N}\frac{\tilde{c}_n}{s-\bar{a}}s^2+s^2\end{bmatrix} \tag{15}$$

where $\sigma(s)$ has a pair of zeros located at zero, i.e., the poles of the rigid body mode. The pole identification problem can be reformulated as

$$\left(\sum_{n=1}^{N}\frac{c_n}{s-\bar{a}}+d+sh\right)-\left(\sum_{n=1}^{N}\frac{\tilde{c}_n}{s-\bar{a}}s^2\right)f(s)=f(s)s^2 \tag{16}$$

The residue identification problem is linearized by the poles calculated from the zeros of $\sigma(s)$

$$f(s)\approx\sum_{n=1}^{N}\frac{c_n}{s-a_n}+h\frac{1}{s^2} \tag{17}$$

Details regarding the pole calculation process can be found in Ref.[15].

2.2 MIMO system vector fitting

The wafer stage identification result is a transfer function matrix, all elements of which have the same pole sets. During the vector fitting process, both the pole identification in Eq. (16) and the residue identification in Eq. (17) lead to an overdetermining problem of the form $\boldsymbol{Ax}=\boldsymbol{b}$ that can be computed by $\boldsymbol{QR}$ decomposition[17]

$$\begin{aligned}&\boldsymbol{A}=\boldsymbol{QR}\\ &\boldsymbol{x}\approx\boldsymbol{R}\backslash(\boldsymbol{Q}^{\mathrm{T}}\boldsymbol{b})\end{aligned} \tag{18}$$

The computation time can be further reduced by applying the $\boldsymbol{QR}$ decomposition to the normal equations instead. Applying the $\boldsymbol{QR}$ decomposition to Eq. (15) transforms the pole identification problem into the following

$$\begin{bmatrix}\boldsymbol{R}_{11}&\boldsymbol{R}_{12}\\ \boldsymbol{0}&\boldsymbol{R}_{22}\end{bmatrix}\begin{bmatrix}\boldsymbol{x}_1\\ \boldsymbol{x}_2\end{bmatrix}=\boldsymbol{Q}^{\mathrm{T}}\begin{bmatrix}\boldsymbol{b}_1\\ \boldsymbol{b}_2\end{bmatrix} \tag{19}$$

where x_2 is the residue of $\sigma(s)$ which is related to the poles. When computing the poles of the frequency response matrix, all equations containing x_2 can be combined as a new equation set. Once the poles of the system are obtained, the SISO system residue identification process (Eq. (17)) can be applied to each matrix element respectively.

The poles and residues can be converted into the state space model[18]. For systems in the rigid body mode such as the transfer function discussed in this paper, the conversion is operated as shown in Fig. 2. A is a diagonal matrix that contains the poles; ones and zeros on the diagonal represent the rigid body mode. C is a matrix containing residues of each element and B is the input matrix containing ones and zeros.

$$\begin{bmatrix} G_{11}(s) & G_{12}(s) \\ G_{21}(s) & G_{22}(s) \end{bmatrix} = \begin{bmatrix} h_{11} & h_{12} \\ h_{21} & h_{22} \end{bmatrix} \frac{1}{s^2} + \begin{bmatrix} r_{1,11} & r_{1,12} \\ r_{1,21} & r_{1,22} \end{bmatrix} \frac{1}{s-p_1} + \begin{bmatrix} r_{2,11} & r_{2,12} \\ r_{2,21} & r_{2,22} \end{bmatrix} \frac{1}{s-p_2} + \cdots + \begin{bmatrix} r_{2n-2,11} & r_{2n-2,12} \\ r_{2n-2,21} & r_{2n-2,22} \end{bmatrix} \frac{1}{s-p_{2n-2}}$$

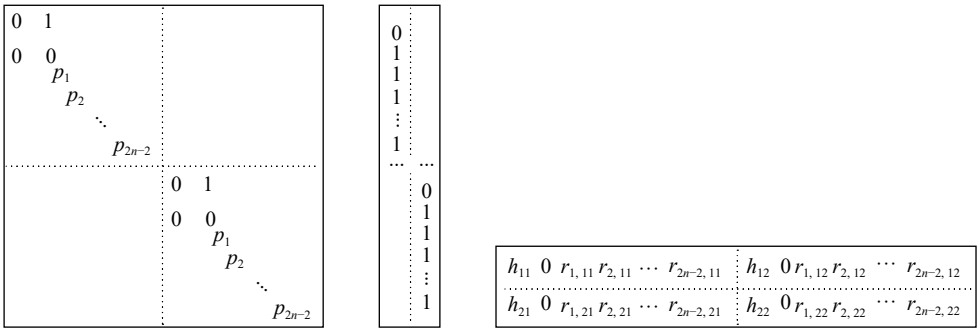

Fig. 2 Transfer function matrix into state space model conversion

3 Experimental Validation

3.1 Setup

Fig.3 shows the structural configuration and real assembly of the flexible stage assessed in this study. The stage is a short stroke of a motion system driven by eight voice coil motors to achieve contactless 6DOF movement.

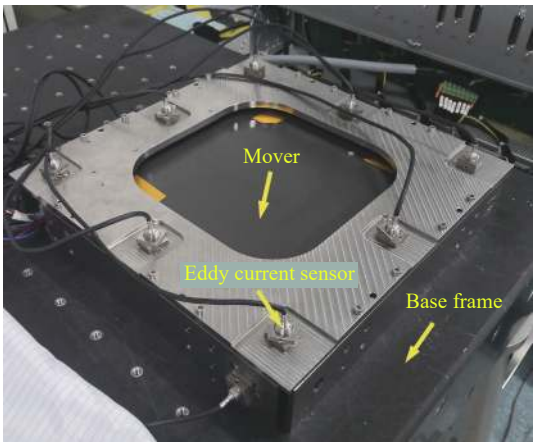

Fig. 3 Experimental wafer stage setup

Four actuators generate driving forces in X and Y directions to realize the planar motion of X, Y, and R_z. The other four actuators in the Z direction realize the motion of R_x, R_y, and Z as well as counteracting gravity. The displacement of the flexible stage is measured with eight eddy sensors, among four control the horizontal DOFs and the other four control the vertical DOFs. The system is decoupled by a displacement calculating matrix and decoupling matrix. The six logical axes are controlled independently by six PID feedback controllers. The system operates in discrete time with a sample time of 200 μs.

3.2 Non-parametric identification

Non-parametric identification is utilized to obtain a frequency response model as the intermediate process for obtaining the transfer function. Feedback is required to ensure stable and safe operation of the wafer stage, so the identification experiment is repeated in a closed-loop configuration (Fig. 4).

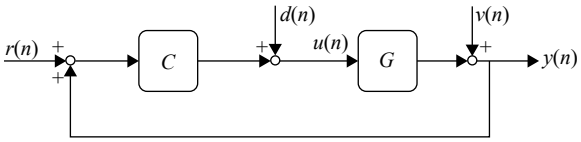

Fig. 4 Closed-loop identification scheme

The open-loop estimation of G can be obtained from the closed-loop frequency response of S_{ud} and S_{yd}:

$$\hat{G}(k) = \widehat{S_{yd}}(k)\,\widehat{S_{ud}}^{-1}(k) \qquad (20)$$

where S_{ud} denotes the FRF matrix estimate from multi-disturbance signal d to multi-input signal u and S_{yd} denotes the FRF matrix estimate from disturbance signal d to output measurement y. S_{yd} and S_{ud} can be obtained using the MIMO open-loop identification method. In this study, they were estimated using the robust multisine approach as described by Pintelon[19-20] to account

for this. Multisine signals are defined as

$$d(n)=\sum A_k \sin\left(2\pi kn/N+\phi_k\right) \tag{21}$$

where N is the number of excited signals, φ_k is the phase angle that is distributed uniformly from 0 to 2π, and A_k denotes the amplitudes of sine waves (identical values). The flexible stage sampling time was 200 μs in this study, so the excitation signals have a wide frequency range from 10 up to 2 500 Hz, which is the Nyqiust frequency of the setup. The N-point discrete Fourier transform of signal u (n) is defined as

$$D_{\mathrm{F}}(k)=\frac{1}{\sqrt{N}}\sum d(n)\mathrm{e}^{-\mathrm{j}2\pi nk/N} \tag{22}$$

The signal as defined in Eqs. (21) (22) excites the single-input system. Full orthogonal signals $n_i\times n_i$ in size were applied to conduct the MIMO identification measurements. They can be described in the frequency domain as

$$\boldsymbol{D}(k)=\boldsymbol{A}_{\mathrm{d}}(k)\boldsymbol{T}\boldsymbol{P}_{\varphi}(k) \tag{23}$$

where $\boldsymbol{A}_{\mathrm{d}}(k)$ is a complex diagonal matrix, the elements of which have random amplitudes and phases; T is an orthogonal matrix and $\boldsymbol{P}_{\varphi}(k)$ is a complex diagonal matrix containing random phase sequences. The excitation signals loaded on the plant can be cycled every 15 periods. The transient response can be mitigated by discarding the first five periods of measurement data from the multisine measurements. The influence of measurement noise is mitigated by averaging the remaining 10 periods' data in the frequency domain.

$$\begin{aligned}\hat{\boldsymbol{Y}}(k)&=\frac{1}{10}\sum_{p=6}^{15}\boldsymbol{Y}_p(k)\\ \hat{\boldsymbol{U}}(k)&=\frac{1}{10}\sum_{p=6}^{15}\boldsymbol{U}_p(k)\end{aligned} \tag{24}$$

The influence of other non-linear behavior was mitigated in this study by averaging eight respective realizations of the $Y(k)$ variable in Eq. (24). The mth matrix of input signals $D^m(k)\in \mathrm{C}_{ni\times ni}$ can then be defined as

$$\boldsymbol{D}^m(k)=\boldsymbol{D}(k)\boldsymbol{T}^m(k) \tag{25}$$

$T^m(k)$ is a unitary matrix containing all the phase information of the input signals. The average over the output signal can be computed as

$$\begin{aligned}\hat{\boldsymbol{Y}}(k)&=\frac{1}{8}\sum_{m=1}^{8}\hat{\boldsymbol{Y}}^m(k)\boldsymbol{T}^{m\mathrm{H}}(k)\\ \hat{\boldsymbol{U}}(k)&=\frac{1}{8}\sum_{m=1}^{8}\hat{\boldsymbol{U}}^m(k)\boldsymbol{T}^{m\mathrm{H}}(k)\end{aligned} \tag{26}$$

Finally, the robust approximation is computed as

$$\begin{aligned}\hat{\boldsymbol{S}}_{yd}(k)&=\hat{\boldsymbol{Y}}(k)\boldsymbol{D}^{-1}(k)\\ \hat{\boldsymbol{S}}_{ud}(k)&=\hat{\boldsymbol{U}}(k)\boldsymbol{D}^{-1}(k)\end{aligned} \tag{27}$$

Blue dotted lines in the Bode diagram presented in Fig. 5 mark the FRF results of the wafer stage. The FRF covers a wide frequency band and shows good quality even at frequencies beyond 1 200 Hz. The Bode diagram of the FRF has a slope of –40 dB at low frequency due to the rigid body mode. The resonance frequency of the first-order flexible mode is 500 Hz and the second is 1 200 Hz, which is consistent with the finite element analysis results. Delays in the hold circuit of the discrete measurement environment had be compensated for during the FRF estimation, then the parametric identification process can be conducted in the continuous time s-domain.

3.3 Parametric identification using modified vector fitting

The parametric modal model is identified using the modified vector fitting (Section 2). The results are also illustrated in Bode diagram form in Fig. 5 as red lines. There is close agreement between the parametric model and the FRF in a wide frequency range (even up to 1 000 Hz). There are some small resonance peaks with frequencies beyond 1 200 Hz introduced by noise in the sensor, which is also modeled in the parametric process. This did not affect the accuracy of the proposed model because this frequency is far higher than the control-loop bandwidth; resonance at these frequencies is hardly excitable.

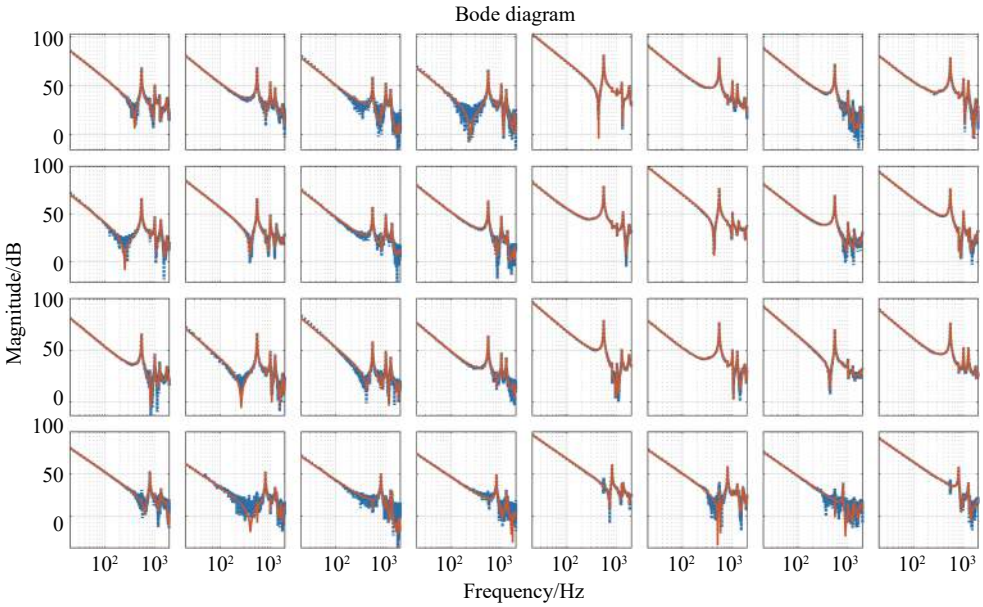

Fig. 5 Wafer stage identification results (4×8 of the 8×8 FRF)

3.4 Model validation

To validate the accuracy of the identified model, its control loop is simulated in Matlab/Simulink software. The control structure diagram is shown in Fig. 6. To ensure the simulation returned the same controller, a position calculation matrix and decoupling matrix were set for the real flexible stage control loop. The disturbance source in the diagram was modeled with the power spectral density (PSD) measured from the output of the PA and sensor, as proposed by Monkhorst[21]. The reference profile of both the real stage and the simulation were set to zero, then the reference error was traced. Fig. 7 shows

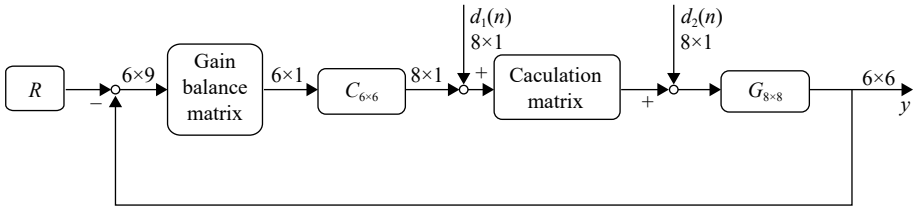

Fig. 6 Simulated control loop scheme

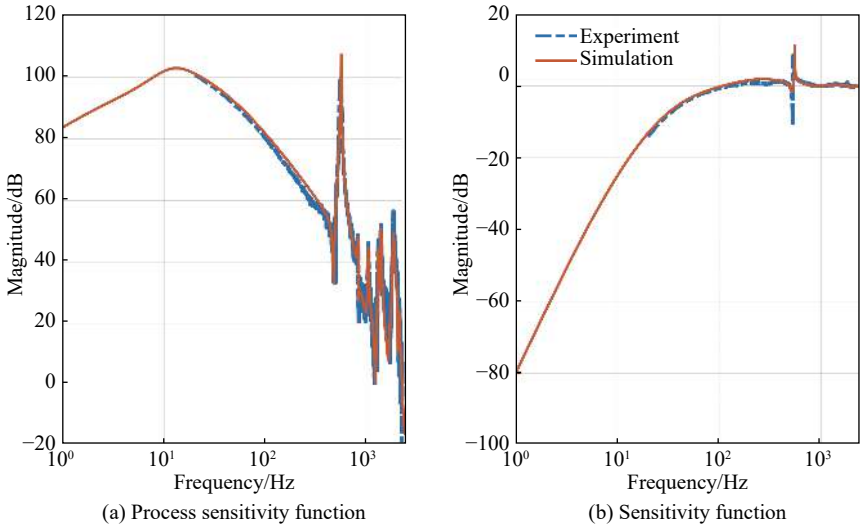

(a) Process sensitivity function (b) Sensitivity function

Fig. 7 Sensitivity function Bode diagram of *Z* axis

the sensitivity and process sensitivity function Bode diagram of the z axis. The simulation results agree closely with the measurement data. When the reference signal is set to zero, the tracking error in the frequency domain is calculated as follows

$$e(k) = S(k)\, d_1(k) + \mathrm{PS}(k)\, d_2(k) \qquad (28)$$

where $S(k)$ is the sensitivity function and $\mathrm{PS}(k)$ is the process sensitivity function. The PSD and cumulative power spectrum (CPS) of the errors are consistent with the measured data when the disturbance source is modeled accurately. Fig. 8 shows the tracking PSD of both the measured and simulated error. The simulated system shows the same servo performance as the real system apart from peaks around 20 Hz which propagated from the floor. These observations are further confirmed by the CPS of the error signal as shown in Fig. 9.

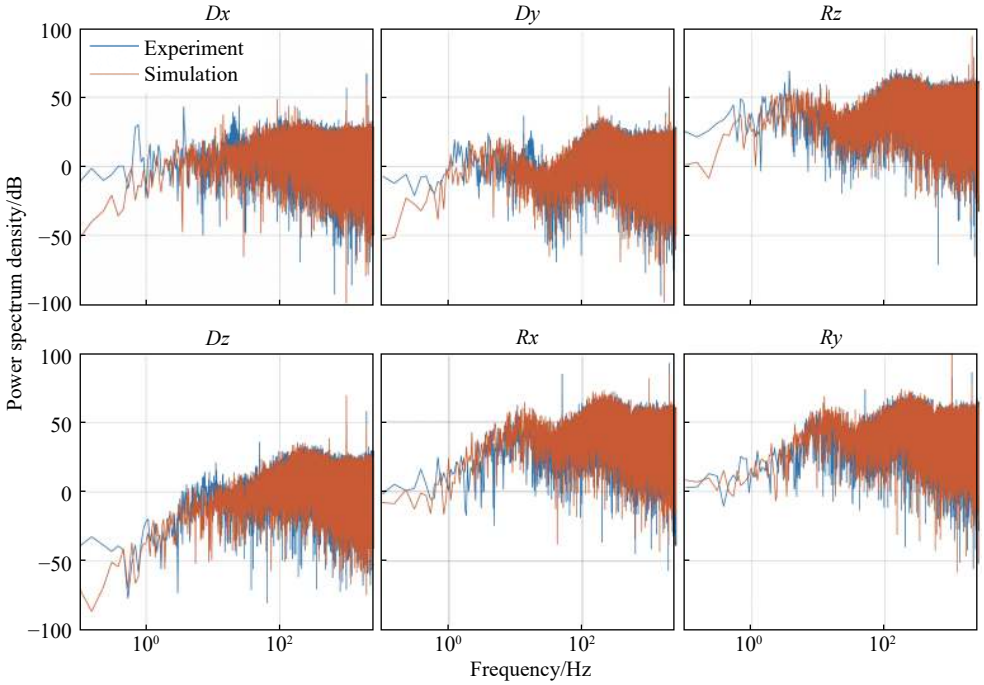

Fig. 8 PSD error

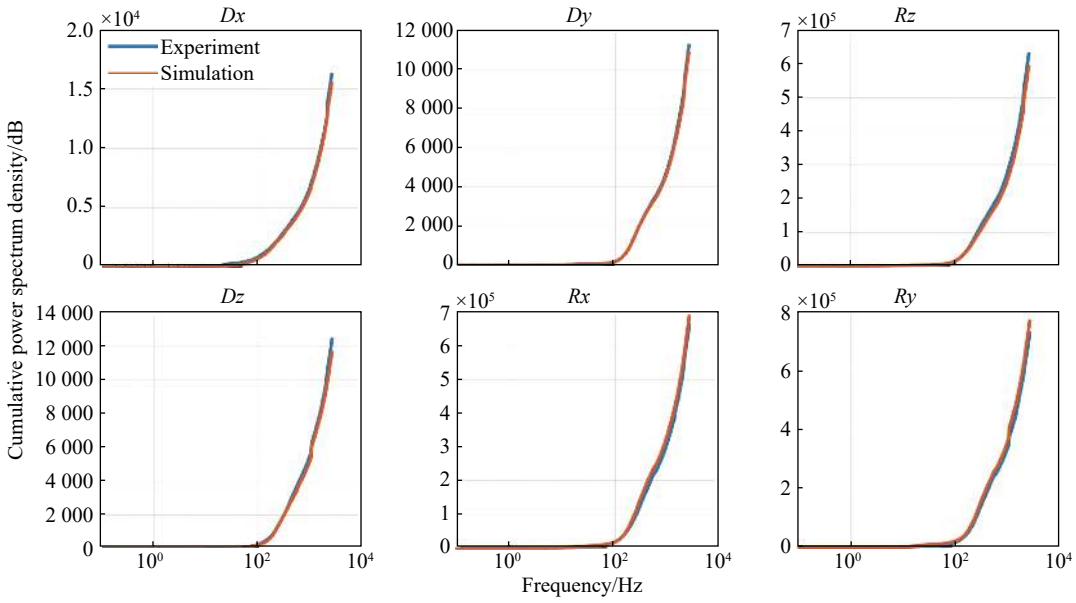

Fig. 9 CPS error

4 Conclusion

A modified vector fitting method is developed in this study for application to parametric identification of models with undamped rigid body modes in frequency domains. The proposed method is tested on the identification of a six-degree-of-freedom (6DOF) wafer stage. The MIMO robust multisine method is applied for non-parametric identification of the stage and provided the accurate FRF of the system; the modal model is then fitted directly from the FRFs. Experimental results show that the model results are in good agreement with FRF data. Simulations are conducted to further validate the accuracy of the proposed fitting model. The power spectrum density and cumulative power spectrum density as-constructed are similar in the simulated system and real control system. To this effect, the proposed identification method is feasible and effective.

References:

[1] Butler H. Position control in lithographic equipment: An enabler for current-day chip manufacturing [J]. IEEE Control Systems Magazine, 2011, 31(5): 28-47.

[2] Oomen T. Advanced motion control for precision mechatronics: Control, identification, and learning of complex systems [J]. IEEJ Journal of Industry Applications, 2018, 7(2): 127-140.

[3] Bruijnen D, Dijk N V. Combined input shaping and feedforward control for flexible motion systems[C]//Proceedings of the American Control Conference, 2012.

[4] Butterworth J A, Pao L Y, Abramovitch D Y. Analysis and comparison of three discrete-time feedforward model-inverse control techniques for nonminimum-phase systems [J]. Mechatronics, 2012, 22(5): 577-587.

[5] Heertjes M, Hennekens D, Engelen A V, et al. Dynamic decoupling in motion systems using a gradient approximation-based algorithm[C]//Proceedings of the 48h IEEE Conference on Decision and Control (CDC) held jointly with 2009 28th Chinese Control Conference, 2009: 5086-5091.

[6] Herpen R V, Oomen T, Kikken E, et al. Exploiting additional actuators and sensors for nano-positioning robust motion control[C]//Proceedings of 2014 American Control Conference, 2014: 984-990.

[7] Oomen T, Grassens E, Hendriks F. Inferential motion control: Identification and robust control framework for positioning an unmeasurable point of interest [J]. IEEE Transactions on Control Systems Technology, 2015, 23(4): 1602-1610.

[8] Dorosti M, Fey R, Heertjes M, et al. Finite element model reduction and model updating of structures for control [J]. IFAC Proceedings Volumes, 2014, 47(3): 4517-4522.

[9] Balas G J, Doyle J C. Identification of flexible structures for robust control [J]. IEEE Control Systems Magazine, 1990, 10(4): 51-58.

[10] Pintelon R, Guillaume P, Rolain Y, et al. Parametric identification of transfer functions in the frequency domain: A survey [J]. IEEE Transactions on Automatic Control, 1994, 39(11): 2245-2260.

[11] Gilson M, Welsh J S, Garnier H. Frequency-domain instrumental variable based method for wide band system identification[C]//Proceedings of the American Control Conference, 2013.

[12] Sanathanan C, Koerner J. Transfer function synthesis as a ratio of two complex polynomials [J]. IEEE Transactions on Automatic Control, 1963, 8(1): 56-58.

[13] Whitfield A H. Asymptotic behaviour of transfer function synthesis methods [J]. International Journal of Control, 1987, 45(3): 1083-1092.

[14] Blom R S, Hof M J V D. Multivariable frequency domain identification using IV-based linear regression[C]//Proceedings of the 49th IEEE Conference on Decision and Control, 2010: 1148-1153.

[15] Gustavsen B, Semlyen A. Rational approximation of frequency domain responses by vector fitting [J]. IEEE Transactions on Power Delivery, 1999, 14(3): 1052-1061.

[16] Gawronski W K. Dynamics and control of structures: A modal approach[M]. Berlin: Springer Science & Business Media, 2004.

[17] Deschrijver D, Mrozowski M, Dhaene T, et al. Macromodeling of multiport systems using a fast implementation of the vector fitting method [J]. IEEE Microwave and Wireless Components Letters, 2008, 18(6): 383-385.

[18] Gustavsen B. Computer code for rational approximation of frequency dependent admittance matrices [J]. IEEE Transactions on Power Delivery, 2002, 17(4): 1093-1098.

[19] Pintelon R, Schoukens J. System identification: A frequency domain approach[M]. 2nd ed. [S. l.]: Wiley-IEEE Press, 2012.

[20] Voorhoeve R, Maas A V D, Oomen T. Non-parametric identification of multivariable systems: A local rational modeling approach with application to a vibration isolation benchmark [J]. Mechanical Systems & Signal Processing, 2018, 105: 129-152.

[21] Monkhorst W. Dynamic error budgeting: A design approach[D]. Delft: Technische Universiteit Delft, 2004.